# Neural Network Control of a Robotic Manipulator With Input Deadzone and Output Constraint

Wei He, *Member, IEEE,* Amoateng Ofosu David, *Student Member, IEEE*, Zhao Yin, *Student Member, IEEE*, and Changyin Sun

***Abstract*—In this paper, we present adaptive neural network tracking control of a robotic manipulator with input deadzone and output constraint. A barrier Lyapunov function is employed to deal with the output constraints. Adaptive neural networks are used to approximate the deadzone function and the unknown model of the robotic manipulator. Both full state feedback control and output feedback control are considered in this paper. For the output feedback control, the high gain observer is used to estimate unmeasurable states. With the proposed control, the output constraints are not violated, and all the signals of the closed loop system are semi-globally uniformly bounded. The performance of the proposed control is illustrated through simulations.**

***Index Terms*—Adaptive control, barrier Lyapunov function, constraints, deadzone, neural networks, robotic manipulator.**

## I. Introduction

ARTIFICIAL neural networks are simple mathematical models of biological neural networks that help in the design of intelligent control systems. Robotic manipulators are among the many motion control systems that are subject to nonlinearities such as deadzone. Nonlinearities are not analytical and it is quite difficult to know their exact models [1]–[3]. Ignoring nonlinearities with the aim of simplifying the control design can lead to steady-state errors, poor transient response, and limited performance during operation [4], [5].

Neural networks have been widely used in the control of robotic manipulators in recent years [6]–[11], because they can approximate the dynamics of the robot and its nonlinearities such as deadzone. In [12], adaptive fuzzy neural networks are used to approximate a nonlinear stochastic system with unknown functions. In [13], radial basis function neural networks are used to approximate the uncertain nonlinear dynamics of a multiagent time delay system. In [14], neural networks are used to propose controllers for a robotic manipulator in the presence of modeling uncertainties and frictional forces. A novel neural network architecture, referred to as a variable neural network, is proposed in [15] to approximate the unknown nonlinearities of a dynamical system. In [16] and [17], neural networks are employed to approximate nonlinear models of friction and backlash hysteresis. In [18], a trajectory tracking controller for a unicycle like mobile robot, including a neural adaptive compensator, is proposed. The radial basis function neural network controller compensates for the difference between a known nominal dynamics structure and the actual dynamics structure of the robot. An adaptive neural network controller for dual-arm co-ordination of a humanoid robot has been proposed in [19]. The controller takes into account unknown output hysteresis nonlinearity and unknown robotic dynamics. In [20] and [21], a higher order neural network is used to design an adaptive controller for a class of uncertain multiple-input multiple-output (MIMO) nonlinear systems.

Some papers, however, consider nonlinear systems without constraints [22]–[29]. Neural networks are just used to approximate the unknown nonlinearities and dynamics of the system. This can degrade system performance when constraints are present in the system. There is, therefore, the need to consider both nonlinearities and constraints in the control design of systems.

There have been quite a number of researches aimed at addressing or tackling the problem of nonlinear systems with input deadzone and output constraint [30]–[35]. In [36], a deadzone compensator is designed for a motion control system using fuzzy logic control. A tuning algorithm is given for a fuzzy logic controller, which guarantees small tracking errors and bounded parameter estimates. In [37], a new iterative learning control for systems with input deadzone is proposed. Through rigorous proof, it is shown that despite the presence of the input deadzone, the simplest iterative learning control scheme retains its ability to achieve the satisfactory performance. A robust nonlinear controller is proposed in [38], to overcome deadzone nonlinearities which are unavoidable in many physical systems due to the imperfections of system components. The proposed control employs an ideal linear model of the system and a model controller to generate an ideal reference output. A nonlinear robust loop controller containing a deadzone is included to force the actual output to follow the ideal reference output. Both simulation and experimental results have shown that the unknown deadzone effects

Manuscript received March 12, 2015; accepted June 13, 2015. Date of publication August 25, 2015; date of current version May 13, 2016. This work was supported in part by the National Natural Science Foundation of China under Grants 61522302, 61125306, and 61520106009, in part by the National Basic Research Program of China (973 Program) under Grant 2014CB744206, and in part by the National High Technology Research and Development Program of China (863 Program) under Grant 2015AA042304. This paper was recommended by Associate Editor Z. Liu.

W. He and C. Sun are with the School of Automation and Electrical Engineering, University of Science and Technology Beijing, Beijing 100083, China (e-mail: weihe@ieee.org).

A. O. David and Z. Yin are with the School of Automation Engineering, University of Electronic Science and Technology of China, Chengdu 611731, China.

Color versions of one or more of the figures in this paper are available online at http://ieeexplore.ieee.org.

Digital Object Identifier 10.1109/TSMC.2015.2466194

2168-2216 © 2015 IEEE. Personal use is permitted, but republication/redistribution requires IEEE permission.
See http://www.ieee.org/publications_standards/publications/rights/index.html for more information.

Authorized licensed use limited to: Indian Institute of Technology - Jodhpur. Downloaded on April 06,2022 at 03:13:47 UTC from IEEE Xplore. Restrictions apply.

are substantially suppressed and satisfactory robust system performance is achieved.

Another method to compensate for the deadzone effect, is by adding in the controller output, an inverse of the deadzone function, to cancel or compensate for the deadzone effect [39]. Deadzone functions are, however, not analytical and therefore not easy to know. Such a controller might not perform well with real life applications. A sliding mode control for uncertain nonlinear systems with multiple inputs with deadzone has been proposed in [40]. In the case of sliding mode control, in order to force the system states to move along the prescribed sliding surface, the control law has to be discontinuous across the sliding surface. With a finite sampling rate this will inevitably lead to chattering [41], [42]. Neural networks are able to approximate the deadzone function suitably. In [43]–[45], neural networks have been used for deadzone compensation. By using tuning algorithms and neural network weights, the neural network deadzone compensation scheme becomes adaptive, resulting in bounded parameter estimates and smaller errors [46]. In [47], an adaptive neural network control algorithm for MIMO nonlinear systems in strict-feedback form are proposed. The unknown functions, the external disturbance, and the unknown deadzone input are considered in the systems. Coordinate transformations are used to transform the systems into a new special form which is suitable for backstepping design technique. The adaptation laws and the controllers are designed based on the transformed systems. The authors have shown that the tracking errors and the adaptation laws are semiglobally uniformly bounded.

To handle output constraints, many techniques have been developed [48]–[50]. Some are based on notions of invariant set theorems using Lyapunov analysis [51], [52]. Position and force control techniques are developed as a means of preventing output violations [53]–[55]. In [53], a force control algorithm is proposed for a robot whose motion is constrained by a point contact between the robot tool and a smooth rigid environment. The force control algorithm utilizes a sliding mode controller and provides asymptotic tracking of the end-effector position and contact force. It is difficult to determine an exact model of a constraint surface in force control applications. A visually adaptive controller is proposed in [54] for motion and force tracking with uncertainties in the constraint surface, kinematics, and dynamics.

An adaptive motion/force control is proposed for nonholonomic robots in [56]. The constraints of the system consist of kinematic constraints for the mobile platform and dynamic constraints for the under-actuated joint. The nonholonomic constraint force between the wheels and the ground is considered in the control design such that the slipping or slippage is avoided during the motion. In [55], an adaptive force/position controller for robotic manipulators during constrained motion has been proposed. The control strategy ensures semiglobal asymptotic tracking performance for the end-effector position and the interaction force between the constraint and the end-effector. A minimum time trajectory planner is proposed in [57]. The planner includes torque joint constraints in order to fully utilize the joint actuators. Other articles and papers have shown that by using a barrier Lyapunov function, constraints demands can be met. The barrier Lyapunov function grows to infinity, whenever it approaches some limits. If the barrier Lyapunov function is kept bounded, then the desired constraint will be met [58]–[60]. The main contributions of this paper include the following.

1) An adaptive neural network controller with both full state and output feedback is proposed to approximate the dynamics and the deadzone nonlinearity of the robotic manipulator.
2) The output violation of the robotic manipulator is prevented by incorporating a barrier Lyapunov function in the controller design.

The rest of this paper is organized as follows. Section II covers the problem formulation and preliminaries using the necessary lemmas, properties and assumptions. The neural network control design with state and output feedback and stability analysis are illustrated in Section III. Section IV shows the simulations of this paper, and Section V concludes this paper.

## II. Problem Formulation and Preliminaries

### A. Problem Formulation

Considering an $n$-link rigid robotic system, the dynamics of the system can be written as [61]

$$M(q)\ddot{q} + C(q, \dot{q})\dot{q} + G(q) + f_{\text{dis}}(t) = D(\tau) \tag{1}$$

where $q \in \mathbb{R}^n$ is the vector of joint displacements, $D(\tau)$ is the deadzone function, $\tau \in \mathbb{R}^n$ is the vector of joint torques supplied by the actuators, $M(q) \in \mathbb{R}^{n\times n}$ is the symmetric positive definite inertia matrix, $C(q, \dot{q}) \in \mathbb{R}^{n\times n}$ is the Coriolis and centrifugal matrix, $G(q) \in \mathbb{R}^n$ is the gravitational force and $f_{\text{dis}}(t) \in \mathbb{R}^n$ represents an external disturbance to the manipulator.

*Property 1 [43]:* The inertia matrix $M(q)$ is symmetric and positive definite.

*Property 2 [43]:* The matrix $\dot{M} - 2C(q, \dot{q})$ is skew-symmetric.

The deadzone nonlinearity can be expressed as [62]

$$D(\tau) = \begin{cases} h_r(\tau - b_r), & \tau \geq b_r \\ 0, & b_l < \tau < b_r \\ h_l(\tau - b_r), & \tau \leq b_l \end{cases} \tag{2}$$

where $\tau$ is the input to the deadzone, $b_l$ and $b_r$ are unknown parameters of the deadzone, $h_r(\cdot)$ and $h_l(\cdot)$ are functions of the deadzone, which are unknown. Fig. 1 shows the structure of the dead zone model.

The control objective is to design an adaptive neural network controller for the robotic system so that it follows a desired trajectory, while the output is bounded. The following assumptions will help achieve our control objective.

*Assumption 1 [63]:* We assume that the disturbance $f_{\text{dis}}$ is uniformly bounded, i.e., there exists a constant $\bar{f} \in \mathbb{R}^+$, such that $|f_{\text{dis}}| \leq \bar{f}$, $\forall t \in [0, \infty)$.

*Assumption 2 [62]:* The desired trajectory is known, continuous and bounded.

*Assumption 3 [62]:* The deadzone parameters, $b_r$ and $b_l$ are unknown constants which satisfy the condition that $b_r > 0$ and $b_l < 0$.

Authorized licensed use limited to: Indian Institute of Technology - Jodhpur. Downloaded on April 06,2022 at 03:13:47 UTC from IEEE Xplore. Restrictions apply.

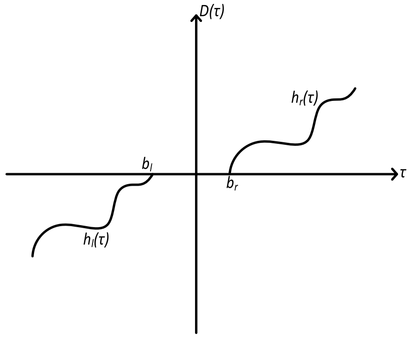


Fig. 1. Deadzone model.

### *B. Technical Lemmas and Definitions*

*Definition 1 [64]:* A barrier Lyapunov function is a scalar function $V(x)$, defined with respect to the system $\dot{x} = f(x)$ on an open region $D$ containing the origin, that is continuous, positive definite, has continuous first-order partial derivatives at every point of $D$, has the property $V(x) \to \infty$ as $x$ approaches the boundary of $D$, and satisfies $V(x(t)) \leq b \; \forall \; t \geq 0$ along the solution of $\dot{x} = f(x)$ for $x(0) \in D$ and some positive constant $b$.

*Lemma 1 [65]:* A Lyapunov function candidate $V(x)$ is bounded if the initial condition $V(0)$ is bounded, $V(x)$ is positive definite and continuous and if

$$\dot{V}(x) \leq -\rho V(x) + C \tag{3}$$

where $\rho > 0$ and $C > 0$.

For output feedback control, some output information may not be measurable. The lemma below is the high gain observer, which will be used to estimate the unmeasurable output.

*Lemma 2 [66]:* Suppose the system output and its first derivatives are bounded, so that $|y^{(k)}| < Y_k$ with a positive constant $Y_k$. Consider the following linear system:

$$\epsilon \dot{\pi}_i = \pi_{i+1}, \quad i = 1, \ldots n-1 \tag{4}$$

$$\epsilon \dot{\pi}_n = -\bar{\lambda}_1 \pi_n - \bar{\lambda}_2 \pi_{n-1} - \cdots - \bar{\lambda}_{n-1} \pi_2 - \pi_1 + x_1(t) \tag{5}$$

where $\epsilon$ is any small positive constant and the terms $\bar{\lambda}_1$ to $\bar{\lambda}_{n-1}$ are chosen such that $s^n + \bar{\lambda}_1 s^{n-1} + \cdots + \bar{\lambda}_{n-1} s + 1$ is Hurwitz. Then the following property is valid:

$$\xi_k = \frac{\pi_k}{\epsilon^{k-1}} - x_1^{(k-1)} = -\epsilon \psi^{(k)}, k = 1, \ldots, n-1 \tag{6}$$

where $\psi = \pi_n + \bar{\lambda}_{n-1} + \cdots + \bar{\lambda}_{n-1} \pi_1$ with $\xi_{(k)}$ denoting the $k^{(th)}$ derivative of $\xi$. Also, $\exists \; t^* > 0$ and $h_k > 0$ which only depends on $Y_k$, $\epsilon$ and $\bar{\lambda}_i$, $i = 1, 2, \ldots, n-1$ such that $\forall \; t > t^*$ we have $|\psi^{(k)}| \leq h_k$, $k = 2, 3, \ldots, n$.

*Lemma 3 [67]:* The basis function of the Gaussian radial basis function neural network with $\hat{X} = X - \gamma \psi$ being the input vector, where $\psi$ is a bounded vector and $\gamma$ is positive is given as

$$s_k(\hat{X}) = \exp\left[\frac{-\left(\hat{X} - \mu_k\right)^T \left(\hat{X} - \mu_k\right)}{\eta_k^2}\right], k = 1, 2, \ldots n \tag{7}$$

$$S(\hat{X}) = S(X) + \gamma S_t \tag{8}$$

where $S_t$ is a bounded vector function.

*Lemma 4 [59]:* For any positive constant vector $b \in \mathbb{R}^n$, the following inequality holds for any vector $x \in \mathbb{R}^n$ in the interval $|x| < |b|$:

$$\ln \frac{b^T b}{b^T b - x^T x} \leq \frac{x^T x}{b^T b - x^T x}. \tag{9}$$

## III. CONTROL DESIGN

Both state feedback and output feedback control schemes are presented in this section. For full state feedback control, we assume the system states, $x_1$ and $x_2$ are known. The adaptive neural network, is used to approximate the unknown dynamics of the robot and the deadzone. For output feedback control, $x_2$ cannot be measured. The high gain observer is used to estimate $x_2$.

### *A. Full State Feedback Control*

We first consider the case where full state information $x_1$ and $x_2$ are available. From (1), if we let $x_1 = [q_1, q_2, \ldots, q_n]^T$ and $x_2 = [\dot{q}_1, \dot{q}_2, \ldots, \dot{q}_n]^T$, the dynamics of the robotic manipulator can be expressed as

$$\dot{x}_1 = x_2 \tag{10}$$

$$\dot{x}_2 = M^{-1}[D(\tau) - C(x_1, x_2)x_2 - f_{\text{dis}} - G(x_1)]. \tag{11}$$

The error variable $e_1$ is defined as

$$e_1 = x_1 - x_d \tag{12}$$

where $x_d$ is the desired trajectory. We define the second error variable

$$e_2 = x_2 - \alpha. \tag{13}$$

Its time derivative is

$$\dot{e_2} = \dot{x_2} - \dot{\alpha}. \tag{14}$$

The barrier Lyapunov function chosen is

$$V_1 = \frac{1}{2} \sum_{i=1}^{n} \ln \frac{b_i^2}{b_i^2 - e_{1i}^2}. \tag{15}$$

Its time derivative is given as

$$\dot{V}_1 = \sum_{i=1}^{n} \frac{e_{1i} \dot{e}_{1i}}{b_i^2 - e_{1i}^2} = \sum_{i=1}^{n} \frac{e_{1i}(e_{2i} + \alpha_i - \dot{x}_{di})}{b_i^2 - e_{1i}^2} \tag{16}$$

we can choose the virtual control $\alpha$ as

$$\alpha = -\begin{bmatrix} k_1 e_{11} - \dot{x}_{d1} \\ k_2 e_{12} - \dot{x}_{d2} \\ \vdots \\ k_n e_{1n} - \dot{x}_{dn} \end{bmatrix}. \tag{17}$$

Substituting (17) into (16) yields

$$\dot{V}_1 = -\sum_{i=1}^{n} \frac{k_i e_{1i}^2}{b_i^2 - e_{1i}^2} + \sum_{i=1}^{n} \frac{e_{1i} e_{2i}}{b_i^2 - e_{1i}^2}. \tag{18}$$

Choosing a second Lyapunov function candidate as

$$V_2 = V_1 + \frac{1}{2} e_2^T M(x_1) e_2. \tag{19}$$

Authorized licensed use limited to: Indian Institute of Technology - Jodhpur. Downloaded on April 06,2022 at 03:13:47 UTC from IEEE Xplore. Restrictions apply.

Its derivative yields

$$\dot{V}_2 = \dot{V}_1 + e_2^T M(x_1)\dot{e}_2 + e_2^T \frac{1}{2}\dot{M}(x_1)e_2. \quad (20)$$

Substituting (14) into (20) leads to

$$\dot{V}_2 = \dot{V}_1 + e_2^T\left[M(x_1)(\dot{x}_2 - \dot{\alpha}) + \frac{1}{2}\dot{M}(x_1)e_2\right]. \quad (21)$$

Substituting (11) and (13) into (21) results in

$$\dot{V}_2 = \dot{V}_1 + e_2^T\Big[D(\tau) - f_{\text{dis}} - G(x_1) - C(x_1, x_2)\alpha - M(x_1)\dot{\alpha} + \frac{1}{2}(\dot{M}(x_1) - 2C(x_1, x_2))e_2\Big]. \quad (22)$$

Applying Property 1, (22) is simplified as

$$\dot{V}_2 = \dot{V}_1 + e_2^T[D(\tau) - f_{\text{dis}} - G(x_1) - C(x_1, x_2)\alpha - M(x_1)\dot{\alpha}]. \quad (23)$$

Substituting (18) into (23) and letting $D(\tau) = \tau - \Delta\tau$, $\Delta\tau$ is the error, results in

$$\dot{V}_2 = -\sum_{i=1}^{n}\frac{k_i e_{1i}^2}{b_i^2 - e_{1i}^2} + \sum_{i=1}^{n}\frac{e_{1i}e_{2i}}{b_i^2 - e_{1i}^2} + e_2^T \left[\tau - \Delta\tau - f_{\text{dis}} - G(x_1) - C(x_1, x_2)\alpha - M(x_1)\dot{\alpha}\right]. \quad (24)$$

We design the model-based control as

$$\tau = -K_2 e_2 - \begin{bmatrix} \frac{e_{11}}{b_1^2 - e_{11}^2} \\ \frac{e_{12}}{b_2^2 - e_{12}^2} \\ \vdots \\ \frac{e_{1n}}{b_n^2 - e_{1n}^2} \end{bmatrix} + C(x_1, x_2)\alpha + \Delta\tau + G(x_1) + M(x_1)\dot{\alpha_1} + f_{\text{dis}} \quad (25)$$

where $\dot{\alpha}$ is given as [64]

$$\dot{\alpha} = \sum_{i=1}^{n-1}\frac{\delta\alpha}{\delta x_1}x_i + \sum_{i=0}^{n-1}\frac{\delta\alpha}{\delta {x_d}^i}x_d^{i+1} \quad (26)$$

substituting (25) into (24) results in

$$\dot{V}_2 = -\sum_{i=1}^{n}\frac{k_i e_{1i}^2}{b_i^2 - e_{1i}^2} - e_2^T K_2 e_2 \quad (27)$$

where the gains $k_i > 0$ and $K_2 = K_2^T > 0_{n\times n}$. However, most of these terms such as $\Delta\tau$, $M$, $C$ are unknown. A radial basis function neural network will be used to approximate these. We propose the controller as

$$\tau = -K_2 e_2 - e_2 - \begin{bmatrix} \frac{e_{11}}{b_1^2 - e_{11}^2} \\ \frac{e_{12}}{b_2^2 - e_{12}^2} \\ \vdots \\ \frac{e_{1n}}{b_n^2 - e_{1n}^2} \end{bmatrix} + \hat{W}^T S(X) + \hat{W}_\tau^T S(X_\tau). \quad (28)$$

The network updating law is designed as

$$\dot{\hat{W}}_i = -\Gamma_i\Big(S_i(X)e_{2i} + \sigma_i\hat{W}_i\Big) \quad (29)$$

$$\dot{\hat{W}}_{\tau,j} = -\Gamma_{\tau,j}\Big(S_{\tau,j}(X_\tau)e_{2j} + \sigma_{\tau,j}\hat{W}_{\tau,j}\Big). \quad (30)$$

$\hat{W}^T S(X)$ and $\hat{W}_\tau^T S(X_\tau)$ are used to approximate $W^{*T}S(X)$ and $W_\tau^{*T}S(X_\tau)$, which are given as

$$W^{*T}S(X) = C(x_1, x_2)\alpha + G(x_1) + M(x_1)\dot{\alpha} - \epsilon \quad (31)$$

$$W_\tau^{*T}S(X_\tau) = \Delta\tau - \epsilon_\tau \quad (32)$$

where $W^{*T}$ and $W_\tau^{*T}$ are the ideal neural network weights, $\epsilon$ and $\epsilon_\tau$ are approximation errors of the neural network and $X = [x_1^T, x_2^T, \alpha_1^T, \dot{\alpha_1}^T]^T$ and $X_\tau = [\tau^T, x_1^T, x_2^T, \alpha_1^T]^T$. Substituting (28), (31), and (32) into (24) yields

$$\dot{V}_2 = -e_2^T K_2 e_2 - e_2^T e_2 - e_2^T f_{\text{dis}} - e_2^T\epsilon - e_2^T\epsilon_\tau + e_2^T(\tilde{W}^T S(X) + \tilde{W}_\tau^T S(X_\tau)) - \sum_{i=1}^{n}\frac{k_i e_{1i}^2}{b_i^2 - e_{1i}^2} \quad (33)$$

where $-e_2^T f_{\text{dis}} \le e_2^T e_2 + (1/4)f_{\text{dis}} \le e_2^T e_2 + (1/4)\bar{f}$, then, we have

$$\dot{V}_2 = -e_2^T K_2 e_2 + \frac{1}{4}\bar{f} - e_2^T\epsilon - e_2^T\epsilon_\tau - \sum_{i=1}^{n}\frac{k_i e_{1i}^2}{b_i^2 - e_{1i}^2} + e_2^T(\tilde{W}^T S(X) + \tilde{W}_\tau^T S(X_\tau)) \quad (34)$$

where $\tilde{W} = \hat{W} - W^*$, $\tilde{W}_\tau = \hat{W}_\tau - W_\tau^*$. The Lyapunov function candidate below is suggested, considering the effect of $\tilde{W}$ and $\tilde{W}_\tau$ on system stability

$$V_3 = V_2 + \frac{1}{2}\sum_{i=1}^{n}\tilde{W}_i^T\Gamma_i^{-1}\tilde{W}_i + \frac{1}{2}\sum_{j=1}^{n}\tilde{W}_{\tau,j}^T\Gamma_{\tau,j}^{-1}\tilde{W}_{\tau,j}. \quad (35)$$

Differentiating $V_3$ with respect to time yields

$$\dot{V}_3 = \dot{V}_2 + \sum_{i=1}^{n}\tilde{W}_i^T\Gamma_i^{-1}\dot{\hat{W}}_i + \sum_{j=1}^{n}\tilde{W}_{\tau,j}^T\Gamma_{\tau,j}^{-1}\dot{\hat{W}}_{\tau,j}. \quad (36)$$

Substituting (29), (30), and (33) into (36) and applying Lemma 4 results in

$$\dot{V}_3 \le -e_2^T K_2 e_2 - e_2^T\epsilon - e_2^T\epsilon_\tau + \frac{1}{4}\bar{f} - \sum_{i=1}^{n}\sigma_i\tilde{W}_i^T\hat{W}_i - \sum_{j=1}^{n}\sigma_{\tau,j}\tilde{W}_{\tau,j}^T\hat{W}_\tau, j - \sum_{i=1}^{n}k_i\ln\frac{b_i^2}{b_i^2 - e_{1i}^2}$$

since $-\tilde{W}^T\hat{W} = -\tilde{W}^T(W^* + \tilde{W}) = -\tilde{W}^T\tilde{W} - \tilde{W}^T W^*$ and $-\tilde{W}^T W^* \le (1/2)(\tilde{W}^T\tilde{W} + W^{*T}W^*)$. It simply implies $-\tilde{W}^T\hat{W} \le -(1/2)\tilde{W}^T\tilde{W} + (1/2){W^*}^T W^*$. Also $-e_2^T\epsilon - e_2^T\epsilon_\tau \le e_2^T e_2 + (1/2)\|\epsilon\|^2 + (1/2)\|\epsilon_\tau\|^2$ implies

$$\begin{aligned}\dot{V}_3 &\le -e_2^T(K_2 - I)e_2 + \frac{1}{2}\|\epsilon\|^2 + \frac{1}{2}\|\epsilon_\tau\|^2 + \frac{1}{4}\bar{f} \\ &\quad - \sum_{i=1}^{n}\frac{\sigma_i}{2}\Big(\|\tilde{W}_i\|^2 - \|W_i^*\|^2\Big) \\ &\quad - \sum_{j=1}^{n}\frac{\sigma_{\tau,j}}{2}\Big(\|\tilde{W}_{\tau,j}\|^2 - \|W_{\tau,j}^*\|^2\Big) \\ &\quad - \sum_{i=1}^{n}k_i\ln\frac{b_i^2}{b_i^2 - e_{1i}^2} \\ &\le -\rho V_3 + C \end{aligned} \quad (37)$$

Authorized licensed use limited to: Indian Institute of Technology - Jodhpur. Downloaded on April 06,2022 at 03:13:47 UTC from IEEE Xplore. Restrictions apply.

where

$$\rho = \min\left\{2\min(k_i), \frac{2\lambda_{\min}(K_2 - I)}{\lambda_{\max}(M)}, \frac{\sigma_i}{\Gamma_i^{-1}}, \frac{\sigma_{\tau,j}}{\Gamma_{\tau,j}^{-1}}\right\} \quad (38)$$

$$C = \sum_{i=1}^{n} \frac{\sigma_i}{2}\left\|W_i^*\right\|^2 + \sum_{j=1}^{n} \frac{\sigma_{\tau,j}}{2}\left\|W_{\tau,j}^*\right\|^2 + \frac{1}{2}\|\epsilon\|^2 + \frac{1}{2}\|\epsilon_\tau\|^2 + \frac{1}{4}\bar{f}. \quad (39)$$

To ensure that $\rho > 0$, the gains $k_i$ and $K_2$ are chosen to satisfy

$$\min(k_i) > 0, \quad \lambda_{\min}(K_2 - I) > 0. \quad (40)$$

It can be shown that $e_1, e_2$, and $W$ are semi-globally uniformly bounded. Fig. 2 shows the control strategy for the state feedback control.

*Remark 1:* If $C$ is equal to zero, we can say that the system could achieve exponential stability. However, for our controller, $C = (1/2)\|\epsilon\|^2 + (1/2)\|\epsilon_\tau\|^2 + \sum_{i=1}^{n}(\sigma_i/2)\|W_i^*\|^2 + \sum_{j=1}^{n}(\sigma_{\tau,j}/2)\|W_{\tau,j}^*\|^2 + (1/4)\bar{f}$, where $\sigma_i$ and $\sigma_{\tau,j}$ are control parameters designed in the adaptive law and which improve the robustness of the system. If $\sigma_i$ and $\sigma_{\tau,j}$ are set to zero, the term left is $(1/2)\|\epsilon\|^2+(1/2)\|\epsilon_\tau\|^2$, which is the approximation error of neural network, which is a positive constant. Therefore, we can achieve stability but not exponential stability.

*Theorem 1:* Consider the robotic manipulator system (1) with unknown disturbance, input deadzone, and output constraint. The proposed state feedback radial basis function neural network control law (28), neural network updating laws (29), (30), and the closed loop signals $e_1$, $e_2$, $\tilde{W}$, and $\tilde{W}_\tau$ are semi-globally bounded. Furthermore, the tracking errors $e_1$, $e_2$ and the weights $\tilde{W}$, $\tilde{W}_\tau$ converge automatically to the compact sets $\Omega_{e_1}$, $\Omega_{e_2}$, $\Omega_{\tilde{W}}$, and $\Omega_{\tilde{W}_\tau}$, respectively, defined by

$$\Omega_{e_1} := \left\{e_1 \in \mathbb{R}^n, \|e_{1i}\| \le \sqrt{b_i^2\left(1 - e^{-D}\right)}\right\} \quad (41)$$

$$\Omega_{e_2} := \left\{e_2 \in \mathbb{R}^n, \|e_{2i}\| \le \sqrt{\frac{D}{\lambda_{\min}(M)}}\right\} \quad (42)$$

$$\Omega_{\tilde{W}} := \left\{\tilde{W} \in \mathbb{R}^n, \|\tilde{W}\| \le \sqrt{\frac{D}{\lambda_{\min}\left(\Gamma^{-1}\right)}}\right\} \quad (43)$$

$$\Omega_{\tilde{W}_\tau} := \left\{\tilde{W} \in \mathbb{R}^n, \left\|\tilde{W}_\tau\right\| \le \sqrt{\frac{D}{\lambda_{\min}\left(\Gamma_\tau^{-1}\right)}}\right\} \quad (44)$$

where $D = 2(V_3(0) + (C/\rho))$. $\rho$ and $C$ are defined in (38) and (39).

*Proof:* The proof of Theorem 1 is shown in the Appendix. ■

### B. Output Feedback Control

In the design of the state feedback control law (28), we assumed that the output states can be measured. It is not practical to assume that all output states can be measured [68], [69]. In this section, we present the output feedback control, which uses the high gain observer to approximate the unmeasurable terms [70]. The unmeasurable state $x_2$ is approximated as $(\pi_2/\epsilon)$ [71]. $e_2$ can, therefore, be estimated as

$$\hat{e}_2 = \frac{\pi_2}{\epsilon} - \alpha \quad (45)$$

where $\pi_2$ is described as

$$\epsilon\dot{\pi}_i = \pi_2 \quad (46)$$

$$\epsilon\dot{\pi}_2 = \lambda_1\pi_2 - \pi_1 + x_1. \quad (47)$$

According to Lemma 2, we have

$$\xi_2 = \frac{\pi_2}{\epsilon} - \dot{x}_1 = -\epsilon\psi^{(2)} \quad (48)$$

$$\tilde{e}_2 = \hat{e}_2 - e_2 = \frac{\pi_2}{\epsilon} - \alpha_1 - \dot{x}_1 + \alpha_1 = \xi_2 \quad (49)$$

where $\epsilon$ is a small constant, $\psi = \pi_2 + \lambda_1\pi_1$ and there exits positive constants $t^*$ and $h_2$ such that $\forall t > t^*$, we have $\|\xi_2\| \le \epsilon h_2$. Therefore, we can use $(\pi_2/\epsilon)$ to estimate $\dot{x}_1$ and $x_2$, $e_2$ can be estimated as follows:

$$\hat{x}_2 = \frac{\pi_2}{\epsilon} \quad (50)$$

$$\hat{e}_2 = \frac{\pi_2}{\epsilon} - \alpha. \quad (51)$$

We can choose the virtual control $\alpha$ as

$$\alpha = -\begin{bmatrix} k_1e_{11} - \dot{x}_{d1} \\ k_2e_{12} - \dot{x}_{d2} \\ \vdots \\ k_ne_{1n} - \dot{x}_{dn} \end{bmatrix}. \quad (52)$$

Substituting (52) into (16) yields

$$\dot{V}_1 = -\sum_{i=1}^{n} \frac{k_ie_{1i}^2}{b_i^2 - e_{1i}^2} + \sum_{i=1}^{n} \frac{e_{1i}e_{2i}}{b_i^2 - e_{1i}^2}. \quad (53)$$

From the state feedback control law (28) and radial basis function neural network updating laws (29), (30) we rewrite the output feedback control law and its updating laws as

$$\tau = -\begin{bmatrix} \frac{e_{11}}{b_1^2-e_{11}^2} \\ \frac{e_{12}}{b_2^2-e_{12}^2} \\ \vdots \\ \frac{e_{1i}}{b_i^2-e_{1i}^2} \end{bmatrix} - K_2\hat{e}_2 - \hat{e}_2 + \hat{W}^TS\left(\hat{X}\right) + \hat{W}_\tau^TS\left(\hat{X}_\tau\right) \quad (54)$$

$$\dot{\hat{W}}_i = -\Gamma_i\left(S_i\left(\hat{X}\right)\hat{e}_{2i} + \sigma_i\hat{W}_i\right) \quad (55)$$

$$\dot{\hat{W}}_{\tau,j} = -\Gamma_{\tau,j}\left(S_{\tau,j}\left(\hat{X}_\tau\right)\hat{e}_{2j} + \sigma_{\tau,j}\hat{W}_{\tau,j}\right). \quad (56)$$

Consider the following Lyapunov function candidate:

$$V_2 = V_1 + \frac{1}{2}e_2^TM(x_1)e_2 + \frac{1}{2}\sum_{i=1}^{n}\tilde{W}_i^T\Gamma_i^{-1}\tilde{W}_i + \frac{1}{2}\sum_{j=1}^{n}\tilde{W}_{\tau,j}^T\Gamma_{\tau,j}^{-1}\tilde{W}_{\tau,j}. \quad (57)$$

Differentiating (57) yields

$$\dot{V}_2 = \dot{V}_1 + e_2^T\left(\tau - f_{\text{dis}} - W^{*T}S(X) - \epsilon - W_\tau^{*T}S_\tau(X_\tau) - \epsilon_\tau\right) + \sum_{i=1}^{n}\tilde{W}_i^T\Gamma_i^{-1}\dot{\hat{W}}_i + \sum_{j=1}^{n}\tilde{W}_{\tau,j}^T\Gamma_{\tau,j}^{-1}\dot{\hat{W}}_{\tau,j}. \quad (58)$$

Authorized licensed use limited to: Indian Institute of Technology - Jodhpur. Downloaded on April 06,2022 at 03:13:47 UTC from IEEE Xplore. Restrictions apply.

Substituting (53)–(56) into (58) yields

$$\begin{aligned}\dot{V}_2 = {} & e_2^T\Big(-K_2\hat{e}_2 - \hat{e}_2 - f_{\text{dis}} + \hat{W}^T S\big(\hat{X}\big) \\ & + \hat{W}_\tau^T S\big(\hat{X}_\tau\big) - W^{*T}S(X) - W_\tau^{*T}S(X_\tau)\Big) \\ & - e_2^T(\epsilon + \epsilon_\tau) - \sum_{i=1}^{n}\tilde{W}_i^T S_i\big(\hat{X}\big)\hat{e}_{2,i} \\ & - \sum_{i=1}^{n}\tilde{W}_i^T\sigma_i\hat{W}_i - \sum_{j=1}^{n}\tilde{W}_{\tau,j}^T S_{\tau,j}(X_\tau)\hat{e}_{2,j} \\ & - \sum_{j=1}^{n}\tilde{W}_{\tau,j}^T\sigma_{\tau,j}\hat{W}_{\tau,j} - \sum_{i=1}^{n}\frac{k_i e_{1i}^2}{b_i^2 - e_{1i}^2}. \end{aligned} \tag{59}$$

Substituting (8) into (59) yields

$$\begin{aligned}\dot{V}_2 = {} & -\sum_{i=1}^{n}\frac{k_i e_{1i}^2}{b_i^2 - e_{1i}^2} - e_2^T K_2\hat{e}_2 + e_2^T e_2 - e_2^T\hat{e}_2 + \frac{1}{4}\bar{f} \\ & + e_2^T\Big[\tilde{W}^T S\big(\hat{X}\big) + \tilde{W}_\tau^T S_\tau\big(\hat{X}_\tau\big)\Big] - e_2^T(\epsilon + \epsilon_\tau) \\ & + e_2^T\big[W_\tau^{*T}(\gamma_\tau S_{\tau t}) + W^{*T}(\gamma S_t)\big] \\ & - \sum_{i=1}^{n}\tilde{W}_i^T S_i\big(\hat{X}\big)\hat{e}_{2,i} - \sum_{i=1}^{n}\tilde{W}_i^T\sigma_i\hat{W}_i \\ & - \sum_{j=1}^{n}\tilde{W}_{\tau,j}^T S_{\tau,j}(X_\tau)\hat{e}_{2,j} - \sum_{j=1}^{n}\tilde{W}_{\tau,j}^T\sigma_{\tau,j}\hat{W}_{\tau,j}. \end{aligned} \tag{60}$$

Defining $\hat{e}_2 = \tilde{e}_2 + e_2$ and substituting it into the above equation yields

$$\begin{aligned}\dot{V}_2 = {} & -\sum_{i=1}^{n}\frac{k_i e_{1i}^2}{b_i^2 - e_{1i}^2} - e_2^T K_2 e_2 - e_2^T K_2\tilde{e}_2 - e_2^T\tilde{e}_2 \\ & - e_2^T(\epsilon + \epsilon_\tau) + \sum_{i=1}^{n}\Big[W_i^{*T}(\gamma S_{ti})e_{2,i} + \frac{1}{4}\bar{f} \\ & \qquad - \tilde{W}_i^T S_i\big(\hat{X}\big)\tilde{e}_{2,i} - \tilde{W}_i^T\sigma_i\hat{W}_i\Big] \\ & + \sum_{j=1}^{n}\Big[W_{\tau,j}^{*T}(\gamma S_{t\tau,j})e_{2,j} - \tilde{W}_i^T S_{\tau,j}\big(\hat{X}\big)\tilde{e}_{2,j} - \tilde{W}_{\tau,j}^T\sigma_{\tau,j}\hat{W}_{\tau,j}\Big]. \end{aligned} \tag{61}$$

However

$$-e_2^T K_2\tilde{e}_2 \le \frac{1}{2}e_2^T e_2 + \frac{1}{2}(K_2\tilde{e}_2)^T(K_2\tilde{e}_2) \tag{62}$$

$$-e_2^T\tilde{e}_2 \le \frac{1}{2}e_2^T e_2 + \frac{1}{2}\tilde{e}_2^T\tilde{e}_2. \tag{63}$$

Also, $-\tilde{W}^T\hat{W} = -\tilde{W}^T(W^* + \tilde{W}) = -\tilde{W}^T\tilde{W} - \tilde{W}^T W^*$ and $-\tilde{W}^T W^* \le (1/2)(\tilde{W}^T\tilde{W} + W^{*T}W^*)$. It simply implies

$$-\tilde{W}_i^T\hat{W}_i \le -\frac{1}{2}\big\|\tilde{W}_i\big\|^2 + \frac{1}{2}\big\|W_i^*\big\|^2 \tag{64}$$

$$-\tilde{W}_{\tau,j}^T\hat{W}_{\tau,j} \le -\frac{1}{2}\big\|\tilde{W}_{\tau,j}\big\|^2 + \frac{1}{2}\Big\|W_{\tau,j}^*\Big\|^2. \tag{65}$$

Moreover

$$-e_2^T\epsilon - e_2^T\epsilon_\tau \le e_2^T e_2 + \frac{1}{2}\|\epsilon\|^2 + \frac{1}{2}\|\epsilon_\tau\|^2 \tag{66}$$

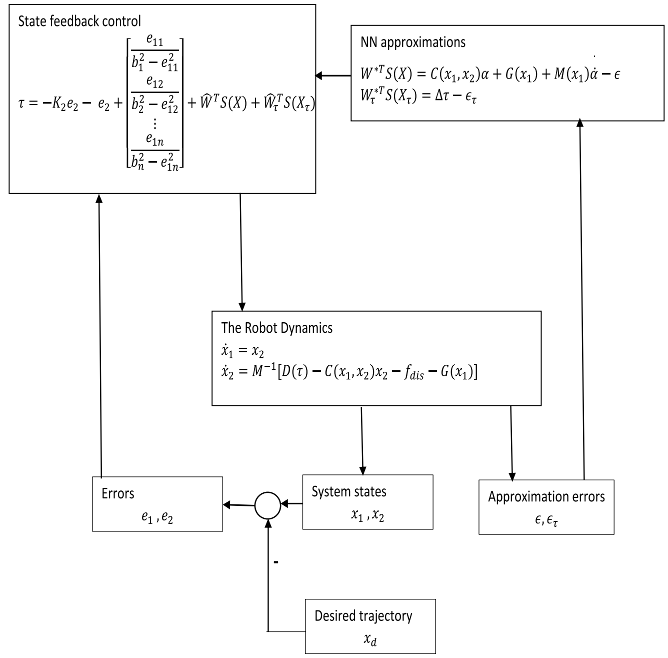


Fig. 2. State feedback control strategy.

$$W_i^*\gamma S_{ti}e_{2,i} \le \frac{1}{2}e_{2,i}^2 + \frac{1}{2}\|\gamma S_{ti}\|^2\big\|W_i^*\big\|^2 \tag{67}$$

$$W_{\tau,j}^*\gamma_\tau S_{t\tau,j}e_{2,i} \le \frac{1}{2}e_{2,i}^2 + \frac{1}{2}\big\|\gamma S_{t\tau,j}\big\|^2\Big\|W_{\tau,j}^*\Big\|^2 \tag{68}$$

$$-\tilde{W}_i^T S_i\big(\hat{X}\big)\tilde{e}_{2,i} \le \frac{\sigma_i}{4}\big\|\tilde{W}_i\big\|^2 + \frac{1}{\sigma_i}\Big\|S_i\big(\hat{X}\big)\Big\|^2\tilde{e}_{2,i}^2 \tag{69}$$

$$\begin{aligned}-\tilde{W}_{\tau,j}^T S_{\tau,j}\big(\hat{X}_\tau\big)\tilde{e}_{2,j} \le {} & \frac{\sigma_{\tau,j}}{4}\big\|\tilde{W}_{\tau,j}\big\|^2 \\ & + \frac{1}{\sigma_{\tau,j}}\Big\|S_{\tau,j}\big(\hat{X}_\tau\big)\Big\|^2\tilde{e}_{2,j}^2. \end{aligned} \tag{70}$$

Substituting $\|S_i(\hat{X}_i)\|^2 \le l_i$ and $\|S_{\tau,j}(\hat{X}_\tau)\|^2 \le l_{\tau,j}$ into (69) and (70) yields

$$-\tilde{W}_i^T S_i\big(\hat{X}\big)\tilde{e}_{2,i} \le \frac{\sigma_i}{4}\big\|\tilde{W}_i\big\|^2 + \frac{2l_i}{\sigma_i}\frac{1}{2}\tilde{e}_{2,i}^2 \tag{71}$$

$$-\tilde{W}_{\tau,j}^T S_{\tau,j}\big(\hat{X}_\tau\big)\tilde{e}_{2,j} \le \frac{\sigma_{\tau,j}}{4}\big\|\tilde{W}_{\tau,j}\big\|^2 + \frac{2l_{\tau,j}}{\sigma_{\tau,j}}\frac{1}{2}\tilde{e}_{2,j}^2. \tag{72}$$

Substituting (62)–(72) into (61) and applying Lemma 4 we have

$$\begin{aligned}\dot{V}_2 \le {} & -\sum_{i=1}^{n}k_i\ln\frac{b_i^2}{b_i^2 - e_{1i}^2} - e_2^T(K_2 - 3)e_2 \\ & - \sum_{i=1}^{n}\frac{\sigma_i}{4}\big\|\tilde{W}_i\big\|^2 - \sum_{j=1}^{n}\frac{\sigma_{\tau,j}}{4}\big\|\tilde{W}_{\tau,j}\big\|^2 \\ & + \sum_{i=1}^{n}\frac{\gamma^2\|S_{ti}\|^2 + \sigma_i}{2}\big\|W_i^*\big\|^2 + \frac{1}{2}\|\epsilon_\tau\|^2 + \frac{1}{4}\bar{f} \\ & + \sum_{j=1}^{n}\frac{\gamma_\tau^2\big\|S_{t\tau,j}\big\|^2 + \sigma_{\tau,j}}{2}\Big\|W_{\tau,j}^*\Big\|^2 + \frac{1}{2}\|\epsilon\|^2 \\ & + \frac{1}{2}\tilde{e}_2^T\big(K_2^T K_2 + \text{diag}[2l_i/\sigma_i] + \text{diag}\big[2l_{\tau,j}/\sigma_{\tau,j}\big] + I\big)\tilde{e}_2. \end{aligned} \tag{73}$$

Authorized licensed use limited to: Indian Institute of Technology - Jodhpur. Downloaded on April 06,2022 at 03:13:47 UTC from IEEE Xplore. Restrictions apply.

Substituting (49) into (73) and applying $(1/2)\xi_2^T\xi_2 \leq (1/2)\epsilon^2 h_2^2$ yields

$$\begin{aligned}\dot{V}_2 \leq & -\sum_{i=1}^{n} k_i \ln \frac{b_i^2}{b_i^2 - e_{1i}^2} - e_2^T(K_2 - 3I)e_2 \\ & -\sum_{i=1}^{n}\frac{\sigma_i}{4}\|\tilde{W}_i\|^2 - \sum_{j=1}^{n}\frac{\sigma_{\tau,j}}{4}\|\tilde{W}_{\tau,j}\|^2 \\ & +\sum_{i=1}^{n}\frac{\gamma^2\|S_{ti}\|^2+\sigma_i}{2}\|W_i^*\|^2 + \frac{1}{2}\|\epsilon_\tau\|^2 + \frac{1}{4}\bar{f} \\ & +\sum_{j=1}^{n}\frac{\gamma_\tau^2\|S_{t\tau,j}\|^2+\sigma_{\tau,j}}{2}\left\|W_{\tau,j}^*\right\|^2 + \frac{1}{2}\|\epsilon\|^2 \\ & +\left(K_2^TK_2 + \mathrm{diag}[2l_i/\sigma_i]\right. \\ & \left. + \mathrm{diag}\left[2l_{\tau,j}/\sigma_{\tau,j}\right] + I\right)\frac{1}{2}\epsilon^2 h_2^2 \\ \leq & -\rho V_2 + C \end{aligned} \tag{74}$$

where $\rho$ and $C$ are defined as

$$\rho = \min\left(2\min(k_i), \frac{2\lambda_{\min}(K_2-3I)}{\lambda_{\max}(M)}, \min_{i=1,2,\ldots n}\left\{\frac{2\sigma_i}{4\lambda_{\max}\left(\Gamma_i^{-1}\right)}\right\} \min_{j=1,2,\ldots n}\left\{\frac{2\sigma_{\tau,j}}{4\lambda_{\max}\left(\Gamma_{\tau,j}^{-1}\right)}\right\}\right) \tag{75}$$

$$\begin{aligned} C = & \sum_{i=1}^{n}\frac{\gamma^2\|S_{ti}\|^2+\sigma_i}{2}\|W_i^*\|^2 \\ & + \left(K_2^TK_2 + \mathrm{diag}[2l_i/\sigma_i] + \mathrm{diag}\left[2l_{\tau,j}/\sigma_{\tau,j}\right] + I\right)\frac{1}{2}\epsilon^2 h_2^2 \\ & + \frac{1}{2}\|\epsilon\|^2 + \frac{1}{2}\|\epsilon_\tau\|^2 + \frac{1}{4}\bar{f} \\ & + \sum_{j=1}^{n}\frac{\gamma_\tau^2\|S_{t\tau,j}\|^2+\sigma_{\tau,j}}{2}\left\|W_{\tau,j}^*\right\|^2. \end{aligned} \tag{76}$$

To ensure $\rho > 0$, the gains $k_i$ and $K_2$ are chosen to satisfy

$$\min(k_i) > 0, \lambda_{\min}(K_2 - 3I) > 0. \tag{77}$$

Fig. 3 shows the control strategy for the output feedback control.

*Remark 2:* If $C$ is equal to zero, we can say that the system could achieve exponential stability. However, for our controller, $C = \sum_{i=1}^{n}(\gamma^2\|S_{ti}\|^2 + \sigma_i/2)\|W_i^*\|^2 + (K_2^TK_2 + \mathrm{diag}[2l_i/\sigma_i] + \mathrm{diag}[2l_{\tau,j}/\sigma_{\tau,j}] + I)(1/2)\epsilon^2h_2^2 + (1/2)\|\epsilon\|^2 + (1/2)\|\epsilon_\tau\|^2 + \sum_{j=1}^{n}(\gamma_\tau^2\|S_{t\tau,j}\|^2 + \sigma_{\tau,j}/2)\|W_{\tau,j}^*\|^2 + (1/4)\bar{f}$, where $\sigma_i$ and $\sigma_{\tau,j}$ are control parameters in the adaptive control law and which improve the robustness of the system. If $\sigma_i$ and $\sigma_{\tau,j}$ are set to zero, there are still some terms left, like errors $(1/2)\|\epsilon\|^2$ and $(1/2)\|\epsilon_\tau\|^2$. Therefore, we can achieve stability but not exponential stability.

*Theorem 2:* Consider the robotic manipulator system (1) with unknown disturbance, input deadzone and output constraint. The proposed output feedback radial basis function

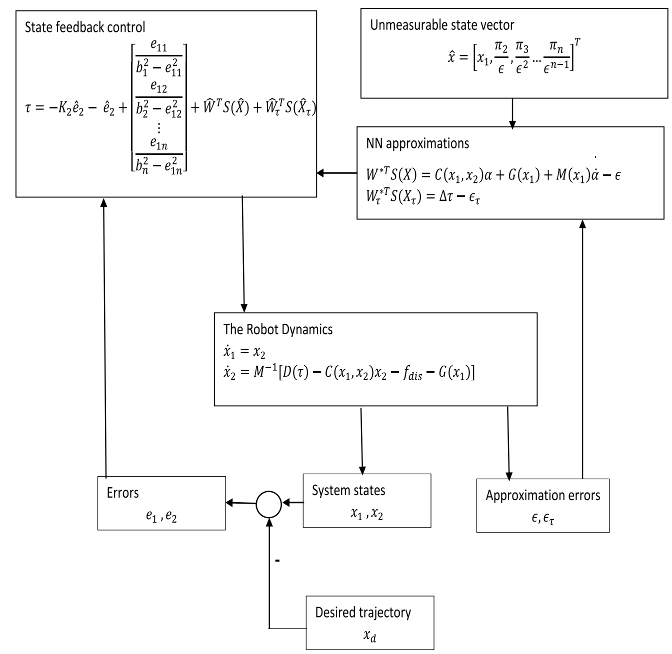


Fig. 3. Output feedback control strategy.

neural network control law (54), neural network updating laws (55), (56), and the closed loop signals $e_1$, $e_2$, $\tilde{W}$, and $\tilde{W}_\tau$ are semi-globally bounded. Furthermore, the tracking errors $e_1$, $e_2$, and the weights $\tilde{W}$, $\tilde{W}_\tau$ converge automatically to the compact sets $\Omega_{e_1}$, $\Omega_{e_2}$, $\Omega_{\tilde{W}}$, and $\Omega_{\tilde{W}_\tau}$, respectively, defined by

$$\Omega_{e_1} := \left\{e_1 \in \mathbb{R}^n, \|e_{1i}\| \leq \sqrt{b_i^2\left(1 - e^{-D}\right)}\right\} \tag{78}$$

$$\Omega_{e_2} := \left\{e_2 \in \mathbb{R}^n, \|e_{2i}\| \leq \sqrt{\frac{D}{\lambda_{\min}(M)}}\right\} \tag{79}$$

$$\Omega_{\tilde{W}} := \left\{\tilde{W} \in \mathbb{R}^n, \|\tilde{W}\| \leq \sqrt{\frac{D}{\lambda_{\min}\left(\Gamma^{-1}\right)}}\right\} \tag{80}$$

$$\Omega_{\tilde{W}_\tau} := \left\{\tilde{W} \in \mathbb{R}^n, \left\|\tilde{W}_\tau\right\| \leq \sqrt{\frac{D}{\lambda_{\min}\left(\Gamma_\tau^{-1}\right)}}\right\} \tag{81}$$

where $D = 2(V_2(0) + (C/\rho))$. $\rho$ and $C$ are defined in (75) and (76).

*Proof:* The proof of Theorem 2 is shown in the Appendix. ■

## IV. Simulation

Through simulations, we verified the effectiveness of our proposed control schemes. A two-DOF robotic manipulator is used for the simulation. The inertia matrix $M(x_1)$, centripetal and coriolis torques $C(x_1, x_2)$ and the gravitational force $G(x_1)$ are expressed as

$$M(x_1) = \begin{bmatrix} M_{11} & M_{12} \\ M_{21} & M_{22} \end{bmatrix} \tag{82}$$

$$C(x_1, x_2) = \begin{bmatrix} C_{11} & C_{12} \\ C_{21} & 0 \end{bmatrix} \tag{83}$$

$$G(x_1) = \begin{bmatrix} G_{11} \\ G_{21} \end{bmatrix} \tag{84}$$

Authorized licensed use limited to: Indian Institute of Technology - Jodhpur. Downloaded on April 06,2022 at 03:13:47 UTC from IEEE Xplore. Restrictions apply.

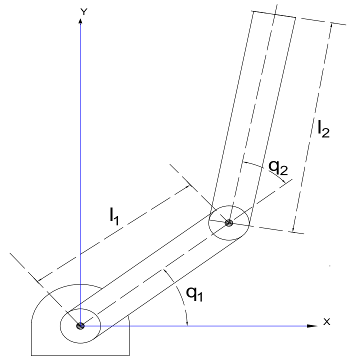


Fig. 4. Diagram of a two-DOF robotic manipulator.

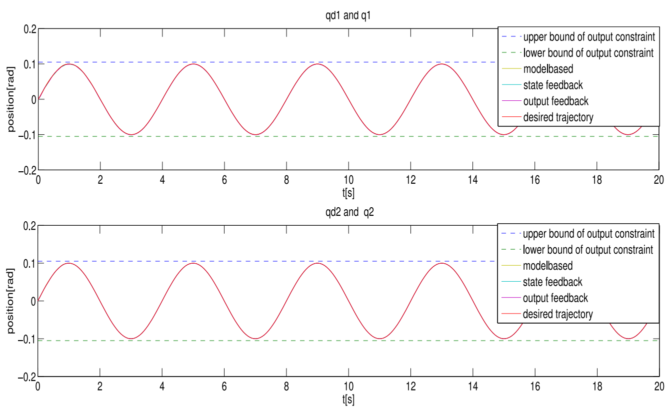


Fig. 5. Tracking performance of constrained controllers at $k_1 = k_2 = 5$ and $K_2 = \text{diag}[5, 5]$.

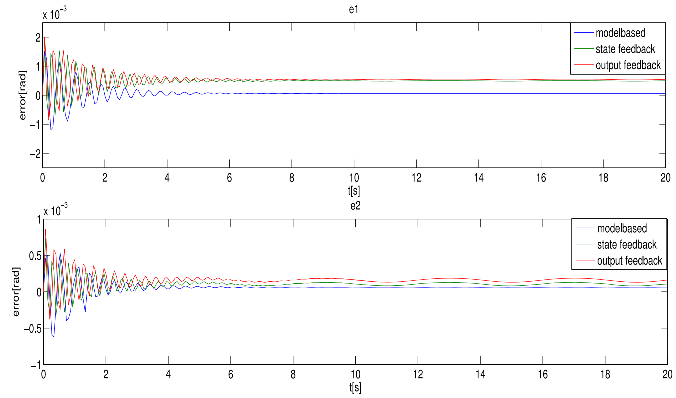


Fig. 6. Error of constrained controllers at $k_1 = k_2 = 5$ and $K_2 = \text{diag}[5, 5]$.

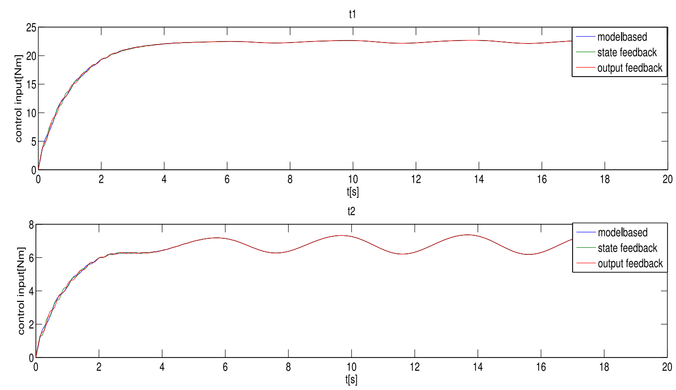


Fig. 7. Torque inputs of constrained controllers.

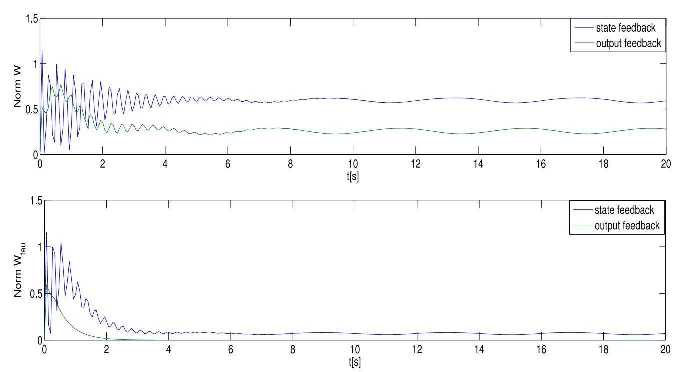


Fig. 8. Norms of radial basis function neural network.

where $M_{11} = m_1 l_1^2 + m_2(l_1^2 + l_2^2 + 2l_1 l_2 \cos q_2)$, $M_{12} = M_{21} = m_2(l_2^2 + l_1 l_2 \cos q_2)$, $M_{22} = m_2 l_2^2$, $C_{11} = -m_2 l_1 l_2 \dot{q}_2 \sin q_2$, $C_{12} = -m_2 l_1 l_2 (\dot{q}_1 + \dot{q}_2) \sin q_2$, $C_{21} = -m_2 l_1 l_2 \dot{q}_1 \sin q_2$, $G_{11} = (m_1 l_2 + m_2 l_1) g \cos q_1 + m_2 l_2 g \cos(q_1 + q_2)$, $G_{21} = m_2 l_2 g \cos(q_1 + q_2)$. Mass of link 1 $m_1 = 1$ kg, mass of link 2 $m_2 = 1$ kg, length of link 1 $l_1 = 0.8$ m, length of link 2 $l_2 = 0.7$ m. The initial positions of the robot is given as $q_0 = [0, 0]$ and $\dot{q}_0 = [0, 0]$. The desired trajectory is chosen as $q_d = [0.1\sin(0.5t), 0.1\sin(0.5t)]$ where $t \in [0, 20]$. Digram of a two-DOF robotic manipulator is shown in Fig. 4.

The robotic manipulator is under external disturbance composed of Gaussian white noise. $f_{\text{dis}}$ is chosen as $1.5[1 - \exp(-0.28t)(\sin(0.5\pi t))]$. The output constraint is set as $b = 0.005$. The unknown deadzone is defined as $b_r = 2.5$ and $b_l = -4.5$, with

$$h_r(\tau) = 2(\tau - b_r)(\sin(\tau) + 1) \tag{85}$$

$$h_l(\tau) = (\tau - b_l)^3. \tag{86}$$

Different cases are considered for the simulation. We examined the model-based control with input deadzone and output constraint proposed in (25), the state feedback control law in (28) and the output feedback control law in (54). We also compare our constrained control schemes with unconstrained ones. Two radial basis function neural networks are used for each case. One is used to compensate for the unknown deadzone function and the other to approximate the unknown dynamics of the robotic manipulator. The control gains are chosen as $k_1 = k_2 = 5$ and $K_2 = \text{diag}[5, 5]$. Sixteen nodes are used with centers chosen in the area of $[-0.5, 0.5] \times [-0.5, 0.5] \times [-0.5, 0.5] \times [-0.5, 0.5]$, $\sigma = 100$, $\Gamma_i = \Gamma_{\tau,j} = 100I$, and $\sigma_i = \sigma_{\tau,j} = 0.02$. The initial weights $\hat{W}_i$ and $\hat{W}_{\tau i} = 0$, $(i = 1, 2, 3, \ldots, 16)$, $\epsilon = 0.0005$, $\lambda = [4, 2]$. The initial conditions of the high gain observer are set as $\pi_1 = \pi_2 = \dot{\pi}_1 = \dot{\pi}_2 = 0$.

The tracking performance of the constrained model based, state feedback and output feedback controllers are shown in Fig. 5. From the figure, it can be seen that all three controllers successfully track the desired trajectory. The controllers also never violate the set constraint. This is because the barrier

Authorized licensed use limited to: Indian Institute of Technology - Jodhpur. Downloaded on April 06,2022 at 03:13:47 UTC from IEEE Xplore. Restrictions apply.

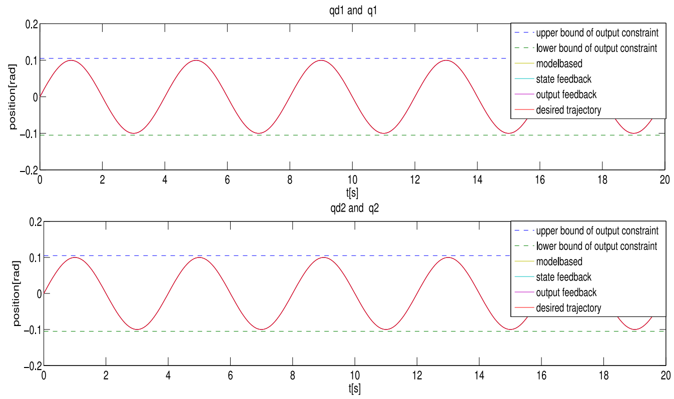


Fig. 9. Tracking performance of constrained controllers at $k_1 = k_2 = 50$ and $K_2 = \text{diag}[50, 50]$.

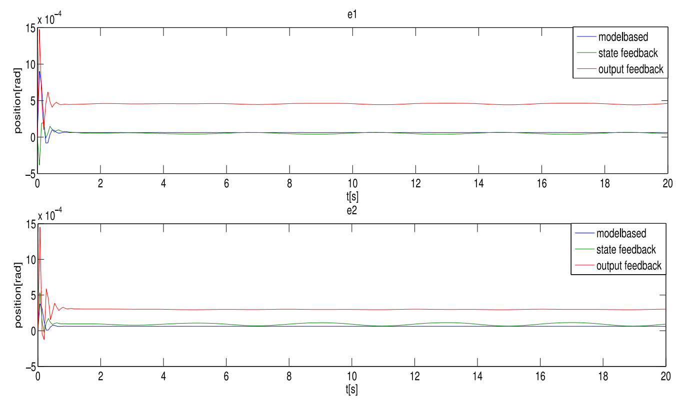


Fig. 10. Error of constrained controllers at $k_1 = k_2 = 50$ and $K_2 = \text{diag}[50, 50]$.

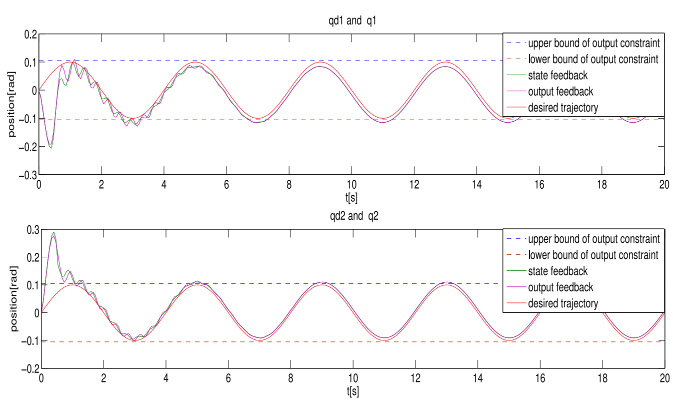


Fig. 11. Tracking performance of unconstrained controllers at $k_1 = k_2 = 5$ and $K_2 = \text{diag}[5, 5]$.

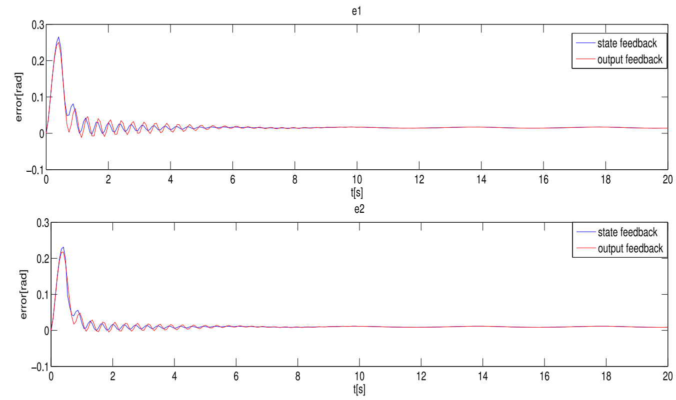


Fig. 12. Error unconstrained of controllers at $k_1 = k_2 = 5$ and $K_2 = \text{diag}[5, 5]$.

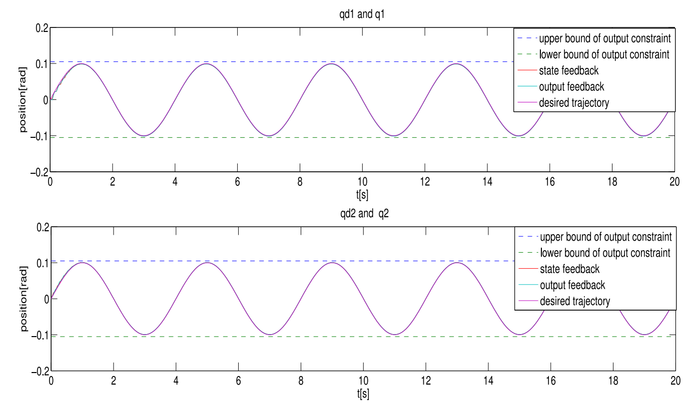


Fig. 13. Tracking performance of unconstrained controllers at $k_1 = k_2 = 50$ and $K_2 = \text{diag}[50, 50]$.

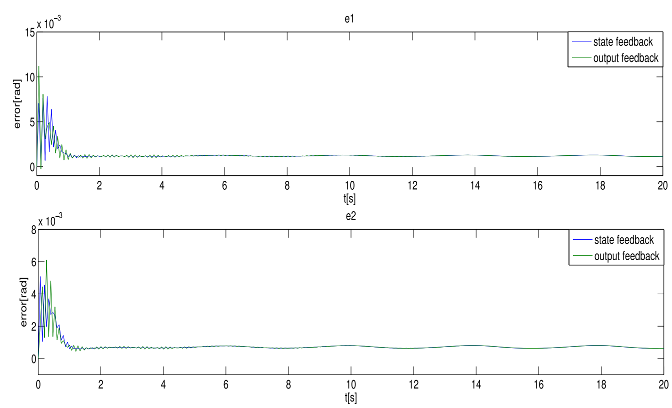


Fig. 14. Error unconstrained of controllers at $k_1 = k_2 = 50$ and $K_2 = \text{diag}[50, 50]$.

Lyapunov function will approach infinity whenever its arguments are approaching the set constraint. Hence, the output states will never violate the set constraint. The system error as shown in Fig. 6, converges to a small value close to zero. The absolute value of the error is always less than 0.005, which is the value of our set constraint. This ensures that our controller is always bounded. The model-based control has the best tracking performance and the least error. This is because it uses dynamics of the robotic manipulator and hence has more information. The state feedback controller also has lesser error than the output feedback controller, because it assumes that all output information is measurable. However, it is not practical to measure all output information. The control gains $k_1$, $k_2$, and $K_2$ are set to 50, 50, and diag[50, 50], respectively. The control inputs and the norm of neural network weights are shown in Figs. 7 and 8 respectively. From Fig. 10, it can be seen that an increase in the gain values made the error signals less oscillatory. The output constraint is also not violated as shown in Fig. 9.

Authorized licensed use limited to: Indian Institute of Technology - Jodhpur. Downloaded on April 06,2022 at 03:13:47 UTC from IEEE Xplore. Restrictions apply.

The performance of the state feedback and output feedback controller, with deadzone compensation but no output constraints is also investigated using the same simulation parameters defined for the constrained controllers. The tracking performance and the error in Figs. 11 and 12 show an unsuccessful tracking of the desired trajectory and also a clear violation of the output constraint. The error overshoots to high value before settling. In a bid to reduce the error and improve the tracking of the unconstrained controller, the gains $k_1$, $k_2$, and $K_2$ are increased to 50, 50, and diag[50, 50], respectively. From Fig. 13, the unconstrained controllers appear to be within bounds of the output constraint. The tracking performance is also better. The error, Fig. 14, is higher than that of the constrained controller even though the unconstrained controller operates at a higher gain value. It is also observed that the external disturbance has negligible impact on all schemes.

## V. Conclusion

In this paper, we have introduced an adaptive neural network to control a robotic manipulator with input deadzone and output constraint. Model based, state feedback and output feedback control have been considered. Simulation results have shown that the constrained controllers have good tracking performance and also keep the output within bounds. Further work includes implementation of the proposed control schemes and control design for the robotic manipulator with other input constraints.

## Appendix

### Proof of Theorem 1

*Proof:* Multiplying (37) by $e^{\rho t}$ yields

$$\frac{d}{dt}\left(V_3 e^{\rho t}\right) \leq C e^{\rho t}. \tag{87}$$

■

Integrating the above inequality, we obtain

$$V_3 \leq \left(V_3(0) - \frac{C}{\rho}\right) e^{-\rho t} + \frac{C}{\rho}. \tag{88}$$

Thus, for $e_1$ we obtain

$$\begin{aligned} \frac{1}{2}\ln\frac{b_i^2}{b_i^2 - e_{1i}^2} &\leq V_3(0) + \frac{C}{\rho} \\ \|e_{1i}\| &\leq \sqrt{b_i^2\left(1 - e^{-D}\right)}. \end{aligned} \tag{89}$$

Similarly for $e_2$, $\tilde{W}$, and $\tilde{W}_\tau$, we obtain

$$\|e_{2i}\| \leq \sqrt{\frac{D}{\lambda_{\min}(M)}} \tag{90}$$

$$\left\|\tilde{W}\right\| \leq \sqrt{\frac{D}{\lambda_{\min}\left(\Gamma^{-1}\right)}} \tag{91}$$

$$\left\|\tilde{W}_\tau\right\| \leq \sqrt{\frac{D}{\lambda_{\min}\left(\Gamma_\tau^{-1}\right)}}. \tag{92}$$

### Proof of Theorem 2

*Proof:* Multiplying (73) by $e^{\rho t}$ yields

$$\frac{d}{dt}\left(V_2 e^{\rho t}\right) \leq C e^{\rho t}. \tag{93}$$

Integrating the above inequality, we have

$$V_2 \leq \left(V_2(0) - \frac{C}{\rho}\right) e^{-\rho t} + \frac{C}{\rho}. \tag{94}$$

Thus, for $e_1$, we obtain

$$\begin{aligned} \frac{1}{2}\ln\frac{b_i^2}{b_i^2 - e_{1i}^2} &\leq V_2(0) + \frac{C}{\rho} \\ \|e_{1i}\| &\leq \sqrt{b_i^2\left(1 - e^{-D}\right)}. \end{aligned} \tag{95}$$

Similarly for $e_2$, $\tilde{W}$ and $\tilde{W}_\tau$, we obtain

$$\|e_{2i}\| \leq \sqrt{\frac{D}{\lambda_{\min}(M)}} \tag{96}$$

$$\left\|\tilde{W}\right\| \leq \sqrt{\frac{D}{\lambda_{\min}\left(\Gamma^{-1}\right)}} \tag{97}$$

$$\left\|\tilde{W}_\tau\right\| \leq \sqrt{\frac{D}{\lambda_{\min}\left(\Gamma_\tau^{-1}\right)}}. \tag{98}$$

■

## Acknowledgment

The authors would like to thank the Editor-in-Chief, the Associate Editor, and the anonymous reviewers for their constructive comments which helped improve the quality and presentation of this paper.

## References

[1] W. Gao and R. Selmic, "Neural network control of a class of nonlinear systems with actuator saturation," *IEEE Trans. Neural Netw.*, vol. 17, no. 1, pp. 147–156, Jan. 2006.
[2] L. Hadjiiski, S. Munster, E. Oesterschulze, and R. Kassing, "Neural network correction of nonlinearities in scanning probe microscope images," *J. Vac. Sci. Technol. B, Microelectron. Nanometer Struct.*, vol. 14, no. 2, pp. 1563–1568, 1996.
[3] R. Selmic and F. Lewis, "Neural-network approximation of piecewise continuous functions: Application to friction compensation," *IEEE Trans. Neural Netw.*, vol. 13, no. 3, pp. 745–751, May 2002.
[4] S. Han and J. Lee, "Output-tracking-error-constrained robust positioning control for a nonsmooth nonlinear dynamic system," *IEEE Trans. Ind. Electron.*, vol. 61, no. 12, pp. 6882–6891, Dec. 2014.
[5] Z. Li, J. Li, and Y. Kang, "Adaptive robust coordinated control of multiple mobile manipulators interacting with rigid environments," *Automatica*, vol. 46, no. 12, pp. 2028–2034, 2010.
[6] L. Wang *et al.*, "Energy-efficient SVM learning control system for biped walking robots," *IEEE Trans. Neural Netw. Learn. Syst.*, vol. 24, no. 5, pp. 831–837, May 2013.
[7] Z. Li and C.-Y. Su, "Neural-adaptive control of single-master-multiple-slaves teleoperation for coordinated multiple mobile manipulators with time-varying communication delays and input uncertainties," *IEEE Trans. Neural Netw. Learn. Syst.*, vol. 24, no. 9, pp. 1400–1413, Sep. 2013.
[8] W. He, Y. Dong, and C. Sun, "Adaptive neural impedance control of a robotic manipulator with input saturation," *IEEE Trans. Syst., Man, Cybern., Syst.*, vol. 46, no. 3, pp. 334–344, Mar. 2016.
[9] C. Yang, Z. Li, and J. Li, "Trajectory planning and optimized adaptive control for a class of wheeled inverted pendulum vehicle models," *IEEE Trans. Cybern.*, vol. 43, no. 1, pp. 24–36, Feb. 2013.

Authorized licensed use limited to: Indian Institute of Technology - Jodhpur. Downloaded on April 06,2022 at 03:13:47 UTC from IEEE Xplore. Restrictions apply.

[10] Z. Li, S. Xiao, S. S. Ge, and H. Su, "Constrained multilegged robot system modeling and fuzzy control with uncertain kinematics and dynamics incorporating foot force optimization," *IEEE Trans. Syst., Man, Cybern., Syst.*, vol. 46, no. 1, pp. 1–15, Jan. 2016.

[11] Z. Li, H. Xiao, C. Yang, and Y. Zhao, "Model predictive control of nonholonomic chained systems using general projection neural networks optimization," *IEEE Trans. Syst., Man, Cybern., Syst.*, vol. 45, no. 10, pp. 1313–1321, Oct. 2015.

[12] C. L. P. Chen, Y.-J. Liu, and G.-X. Wen, "Fuzzy neural network-based adaptive control for a class of uncertain nonlinear stochastic systems," *IEEE Trans. Cybern.*, vol. 44, no. 5, pp. 583–593, May 2014.

[13] C. L. P. Chen, G.-X. Wen, Y.-J. Liu, and F.-Y. Wang, "Adaptive consensus control for a class of nonlinear multiagent time-delay systems using neural networks," *IEEE Trans. Neural Netw. Learn. Syst.*, vol. 25, no. 6, pp. 1217–1226, Jun. 2014.

[14] Y. Kim and F. Lewis, "Optimal design of CMAC neural-network controller for robot manipulators," *IEEE Trans. Syst., Man, Cybern. C, Appl. Rev.*, vol. 30, no. 1, pp. 22–31, Feb. 2000.

[15] G. Liu, V. Kadirkamanathan, and S. Billings, "Variable neural networks for adaptive control of nonlinear systems," *IEEE Trans. Syst., Man, Cybern. C, Appl. Rev.*, vol. 29, no. 1, pp. 34–43, Feb. 1999.

[16] S. Huang and K. K. Tan, "Intelligent friction modeling and compensation using neural network approximations," *IEEE Trans. Ind. Electron.*, vol. 59, no. 8, pp. 3342–3349, Aug. 2012.

[17] D. Seidl, S.-L. Lam, J. Putman, and R. Lorenz, "Neural network compensation of gear backlash hysteresis in position-controlled mechanisms," *IEEE Trans. Ind. Appl.*, vol. 31, no. 6, pp. 1475–1483, Nov./Dec. 1995.

[18] F. Rossomando, C. Soria, and R. Carelli, "Neural network-based compensation control of mobile robots with partially known structure," *IET Control Theory Appl.*, vol. 6, no. 12, pp. 1851–1860, Aug. 2012.

[19] Z. Liu, C. Chen, Y. Zhang, and C. L. P. Chen, "Adaptive neural control for dual-arm coordination of humanoid robot with unknown nonlinearities in output mechanism," *IEEE Trans. Cybern.*, vol. 45, no. 3, pp. 521–532, Mar. 2015.

[20] Y.-J. Liu, C. L. P. Chen, G.-X. Wen, and S.-C. Tong, "Adaptive neural output feedback tracking control for a class of uncertain discrete-time nonlinear systems," *IEEE Trans. Neural Netw.*, vol. 22, no. 7, pp. 1162–1167, Jul. 2011.

[21] Y.-J. Liu, L. Tang, S.-C. Tong, C. L. P. Chen, and D.-J. Li, "Reinforcement learning design-based adaptive tracking control with less learning parameters for nonlinear discrete-time MIMO systems," *IEEE Trans. Neural Netw. Learn. Syst.*, vol. 26, no. 1, pp. 165–176, Jan. 2015.

[22] Z. Liu, G. Lai, Y. Zhang, X. Chen, and C. L. P. Chen, "Adaptive neural control for a class of nonlinear time-varying delay systems with unknown hysteresis," *IEEE Trans. Neural Netw. Learn. Syst.*, vol. 25, no. 12, pp. 2129–2140, Nov. 2014.

[23] Y. Pan, H. Yu, and M. J. Er, "Adaptive neural PD control with semiglobal asymptotic stabilization guarantee," *IEEE Trans. Neural Netw. Learn. Syst.*, vol. 25, no. 12, pp. 2264–2274, Dec. 2014.

[24] B. Xu, Z. Shi, C. Yang, and F. Sun, "Composite neural dynamic surface control of a class of uncertain nonlinear systems in strict-feedback form," *IEEE Trans. Cybern.*, vol. 44, no. 12, pp. 2626–2634, Dec. 2014.

[25] R. Cui, S. S. Ge, V. E. B. How, and Y. S. Choo, "Leader-follower formation control of underactuated autonomous underwater vehicles," *Ocean Eng.*, vol. 37, no. 17, pp. 1491–1502, 2010.

[26] C. Yang, Z. Li, R. Cui, and B. Xu, "Neural network-based motion control of an underactuated wheeled inverted pendulum model," *IEEE Trans. Neural Netw. Learn. Syst.*, vol. 25, no. 11, pp. 2004–2016, Nov. 2014.

[27] B. Xu, C. Yang, and Z. Shi, "Reinforcement learning output feedback NN control using deterministic learning technique," *IEEE Trans. Neural Netw. Learn. Syst.*, vol. 25, no. 3, pp. 635–641, Mar. 2014.

[28] R. Cui, J. Guo, and Z. Mao, "Adaptive backstepping control of wheeled inverted pendulums models," *Nonlin. Dyn.*, vol. 79, no. 1, pp. 501–511, 2015.

[29] N. Wang, M. J. Er, and M. Han, "Parsimonious extreme learning machine using recursive orthogonal least squares," *IEEE Trans. Neural Netw. Learn. Syst.*, vol. 25, no. 10, pp. 1828–1841, Oct. 2014.

[30] Z. Liu, F. Wang, and Y. Zhang, "Adaptive visual tracking control for manipulator with actuator fuzzy dead-zone constraint and unmodeled dynamic," *IEEE Trans. Syst., Man, Cybern., Syst.*, vol. 45, no. 10, pp. 1301–1312, Oct. 2015.

[31] Y.-J. Liu and S.-C. Tong, "Adaptive NN tracking control of uncertain nonlinear discrete-time systems with nonaffine dead-zone input," *IEEE Trans. Cybern.*, vol. 45, no. 3, pp. 497–505, Mar. 2015.

[32] M. Chen, S. S. Ge, and B. How, "Robust adaptive neural network control for a class of uncertain MIMO nonlinear systems with input nonlinearities," *IEEE Trans. Neural Netw.*, vol. 21, no. 5, pp. 796–812, May 2010.

[33] W. He and S. S. Ge, "Vibration control of a flexible beam with output constraint," *IEEE Trans. Ind. Electron.*, vol. 62, no. 8, pp. 5023–5030, Aug. 2015.

[34] W. He, S. Zhang, and S. S. Ge, "Adaptive control of a flexible crane system with the boundary output constraint," *IEEE Trans. Ind. Electron.*, vol. 61, no. 8, pp. 4126–4133, Aug. 2014.

[35] W. He and S. S. Ge, "Vibration control of a flexible string with both boundary input and output constraints," *IEEE Trans. Control Syst. Technol.*, vol. 23, no. 4, pp. 1245–1254, Jul. 2015.

[36] F. Lewis, W. K. Tim, L.-Z. Wang, and Z. Li, "Deadzone compensation in motion control systems using adaptive fuzzy logic control," *IEEE Trans. Control Syst. Technol.*, vol. 7, no. 6, pp. 731–742, Nov. 1999.

[37] J.-X. Xu, J. Xu, and T. H. Lee, "Iterative learning control for systems with input deadzone," *IEEE Trans. Autom. Control*, vol. 50, no. 9, pp. 1455–1459, Sep. 2005.

[38] K. M. Tsang and G. Li, "Robust nonlinear nominal-model following control to overcome deadzone nonlinearities," *IEEE Trans. Ind. Electron.*, vol. 48, no. 1, pp. 177–184, Feb. 2001.

[39] P. L. Andrighetto, A. C. Valdiero, and D. Bavaresco, "Dead zone compensation in pneumatic servo systems," in *Proc. ABCM Symp. Series Mechatronics*, vol. 3. 2008, pp. 501–509.

[40] K.-C. Hsu, W.-Y. Wang, and P.-Z. Lin, "Sliding mode control for uncertain nonlinear systems with multiple inputs containing sector nonlinearities and deadzones," *IEEE Trans. Syst., Man, Cybern. B, Cybern.*, vol. 34, no. 1, pp. 374–380, Feb. 2004.

[41] M. Corradini and G. Orlando, "Robust stabilization of nonlinear uncertain plants with backlash or dead zone in the actuator," *IEEE Trans. Control Syst. Technol.*, vol. 10, no. 1, pp. 158–166, Jan. 2002.

[42] L. Liu, W. Ding, C. Liu, H. Ji, and C. Cao, "Hyperchaos synchronization of fractional-order arbitrary dimensional dynamical systems via modified sliding mode control," *Nonlin. Dyn.*, vol. 76, no. 4, pp. 2059–2071, 2014.

[43] R. Selmic and F. Lewis, "Deadzone compensation in motion control systems using neural networks," *IEEE Trans. Autom. Control*, vol. 45, no. 4, pp. 602–613, Apr. 2000.

[44] B. Xu, "Robust adaptive neural control of flexible hypersonic flight vehicle with dead-zone input nonlinearity," *Nonlin. Dyn.*, vol. 80, no. 3, pp. 1509–1520, 2015.

[45] J. Perez-Cruz, I. Chairez, J. de Jesus Rubio, and J. Pacheco, "Identification and control of class of non-linear systems with non-symmetric deadzone using recurrent neural networks," *IET Control Theory Appl.*, vol. 8, no. 3, pp. 183–192, Feb. 2014.

[46] S. Han and J. Lee, "Precise positioning of nonsmooth dynamic systems using fuzzy wavelet echo state networks and dynamic surface sliding mode control," *IEEE Trans. Ind. Electron.*, vol. 60, no. 11, pp. 5124–5136, Nov. 2013.

[47] Y.-J. Liu, L. Tang, S.-C. Tong, and C. L. P. Chen, "Adaptive NN controller design for a class of nonlinear MIMO discrete-time systems," *IEEE Trans. Neural Netw. Learn. Syst.*, vol. 26, no. 5, pp. 1007–1018, May 2015.

[48] W. He, Y. Chen, and Z. Yin, "Adaptive neural network control of an uncertain robot with full-state constraints," *IEEE Trans. Cybern.*, vol. 46, no. 3, pp. 620–629, Mar. 2016.

[49] W. He, S. S. Ge, and D. Huang, "Modeling and vibration control for a nonlinear moving string with output constraint," *IEEE/ASME Trans. Mechatronics*, vol. 20, no. 4, pp. 1886–1897, Aug. 2015.

[50] W. He, C. Sun, and S. S. Ge, "Top tension control of a flexible marine riser by using integral-barrier Lyapunov function," *IEEE/ASME Trans. Mechatronics*, vol. 20, no. 2, pp. 497–505, Apr. 2015.

[51] J. Lee and S. Han, "Output-tracking-error-constrained robust positioning control for a nonsmooth nonlinear dynamic system," *IEEE Trans. Ind. Electron.*, vol. 61, no. 12, pp. 6882–6891, Dec. 2014.

[52] M. Turner and I. Postlethwaite, "Output violation compensation for systems with output constraints," *IEEE Trans. Autom. Control*, vol. 47, no. 9, pp. 1540–1546, Sep. 2002.

[53] L. Whitcomb, S. Arimoto, T. Naniwa, and F. Ozaki, "Experiments in adaptive model-based force control," *IEEE Control Syst.*, vol. 16, no. 1, pp. 49–57, Feb. 1996.


Authorized licensed use limited to: Indian Institute of Technology - Jodhpur. Downloaded on April 06,2022 at 03:13:47 UTC from IEEE Xplore. Restrictions apply.

[54] C. C. Cheah, S. P. Hou, Y. Zhao, and J.-J. E. Slotine, "Adaptive vision and force tracking control for robots with constraint uncertainty," *IEEE/ASME Trans. Mechatronics*, vol. 15, no. 3, pp. 389–399, Jun. 2010.
[55] M. S. De Queiroz, J. Hu, D. M. Dawson, T. Burg, and S. R. Donepudi, "Adaptive position/force control of robot manipulators without velocity measurements: Theory and experimentation," *IEEE Trans. Syst., Man, Cybern. B, Cybern.*, vol. 27, no. 5, pp. 796–809, Sep. 1997.
[56] Z. Li, Y. Yang, and J. Li, "Adaptive motion/force control of mobile under-actuated manipulators with dynamics uncertainties by dynamic coupling and output feedback," *IEEE Trans. Control Syst. Technol.*, vol. 18, no. 5, pp. 1068–1079, Sep. 2010.
[57] H. Tan and R. Potts, "Minimum time trajectory planner for the discrete dynamic robot model with dynamic constraints," *IEEE J. Robot. Autom.*, vol. 4, no. 2, pp. 174–185, Apr. 1988.
[58] B. Ren, S. S. Ge, K. P. Tee, and T. H. Lee, "Adaptive neural control for output feedback nonlinear systems using a barrier Lyapunov function," *IEEE Trans. Neural Netw.*, vol. 21, no. 8, pp. 1339–1345, Aug. 2010.
[59] Z. Zhao, W. He, and S. S. Ge, "Adaptive neural network control of a fully actuated marine surface vessel with multiple output constraints," *IEEE Trans. Control Syst. Technol.*, vol. 22, no. 4, pp. 1536–1543, Jul. 2014.
[60] X.-J. Wu, X.-L. Wu, X.-Y. Luo, and X.-P. Guan, "Brief paper—Dynamic surface control for a class of state-constrained non-linear systems with uncertain time delays," *IET Control Theory Appl.*, vol. 6, no. 12, pp. 1948–1957, Aug. 2012.
[61] S. S. Ge, C.-C. Hang, and L. Woon, "Adaptive neural network control of robot manipulators in task space," *IEEE Trans. Ind. Electron.*, vol. 44, no. 6, pp. 746–752, Dec. 1997.
[62] J. Campos and F. Lewis, "Deadzone compensation in discrete time using adaptive fuzzy logic," *IEEE Trans. Fuzzy Syst.*, vol. 7, no. 6, pp. 697–707, Dec. 1999.
[63] W. He, S. S. Ge, Y. Li, E. Chew, and Y. S. Ng, "Neural network control of a rehabilitation robot by state and output feedback," *J. Intell. Robot. Syst.*, 2015, vol. 80, no. 1, pp. 15–31, Oct. 2015.
[64] K. P. Tee, S. S. Ge, and E. H. Tay, "Barrier Lyapunov functions for the control of output-constrained nonlinear systems," *Automatica*, vol. 45, no. 4, pp. 918–927, 2009.
[65] S. S. Ge and C. Wang, "Adaptive neural control of uncertain MIMO nonlinear systems," *IEEE Trans. Neural Netw.*, vol. 15, no. 3, pp. 674–692, May 2004.
[66] S. S. Ge and J. Zhang, "Neural-network control of nonaffine nonlinear system with zero dynamics by state and output feedback," *IEEE Trans. Neural Netw.*, vol. 14, no. 4, pp. 900–918, Jul. 2003.
[67] S. S. Ge and J. Wang, "Robust adaptive neural control for a class of perturbed strict feedback nonlinear systems," *IEEE Trans. Neural Netw.*, vol. 13, no. 6, pp. 1409–1419, Nov. 2002.
[68] L. Liu, D. Liang, and C. Liu, "Nonlinear state-observer control for projective synchronization of a fractional-order hyperchaotic system," *Nonlin. Dyn.*, vol. 69, no. 4, pp. 1929–1939, 2012.
[69] Y.-J. Liu, S.-C. Tong, D. Wang, T.-S. Li, and C. L. P. Chen, "Adaptive neural output feedback controller design with reduced-order observer for a class of uncertain nonlinear SISO systems," *IEEE Trans. Neural Netw.*, vol. 22, no. 8, pp. 1328–1334, Aug. 2011.
[70] A. Prasov and H. Khalil, "A nonlinear high-gain observer for systems with measurement noise in a feedback control framework," *IEEE Trans. Autom. Control*, vol. 58, no. 3, pp. 569–580, Mar. 2013.
[71] K. P. Tee and S. S. Ge, "Control of fully actuated ocean surface vessels using a class of feedforward approximators," *IEEE Trans. Control Syst. Technol.*, vol. 14, no. 4, pp. 750–756, Jul. 2006.

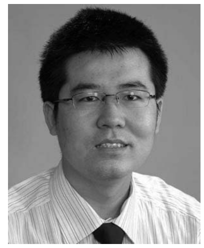

**Wei He** (S'09–M'12) received the B.Eng. degree from the College of Automation Science and Engineering, South China University of Technology, Guangzhou, China, in 2006, and the Ph.D. degree from the National University of Singapore (NUS), Singapore, in 2011.

He was a Research Fellow with the Department of Electrical and Computer Engineering, NUS from 2011 to 2012. He is currently with the School of Automation and Electrical Engineering, University of Science and Technology Beijing, Beijing, China. His current research interests include robotics, distributed parameter systems, and intelligent control systems.

Dr. He serves as an Editor of the *Journal of Intelligent and Robotic Systems* (Springer).

**Amoateng Ofosu David** (S'15) received the B.Sc. degree in electrical and electronic engineering from the Kwame Nkrumah University of Science and Technology, Kumasi, Ghana, in 2013. He is currently pursuing the M.Sc. degree with the School of Automation Engineering, University of Electronic Science and Technology of China, Chengdu, China.

His current research interests include neural networks, adaptive control, and robotics.

**Zhao Yin** (S'14) received the B.Eng. degree in electric engineering and automation from Hangzhou Dianzi University, Zhejiang, China, in 2013. He is currently pursuing the M.Eng. degree with the School of Automation Engineering, University of Electronic Science and Technology of China, Chengdu, China.

His current research interests include neural network control, adaptive control, and robotics.

**Changyin Sun** received the M.S. and Ph.D. degrees in electrical engineering from Southeast University, Nanjing, China, in 2001 and 2003, respectively.

He is a Professor with the School of Automation and Electrical Engineering, University of Science and Technology Beijing, Beijing, China. His current research interests include intelligent control, flight control, pattern recognition, and optimal theory.

Authorized licensed use limited to: Indian Institute of Technology - Jodhpur. Downloaded on April 06,2022 at 03:13:47 UTC from IEEE Xplore. Restrictions apply.